ECOLOGICAL ENGINEERING & ENVIRONMENTAL TECHNOLOGY

Ecological Engineering & Environmental Technology, 2026, 27(9), 424–441
https://doi.org/10.12912/27197050/226549
ISSN 2719–7050, License CC-BY 4.0

Received: 2026.07.12
Accepted: 2026.08.03
Published: 2026.08.15

Assessment of future temperature and precipitation variability in southern Iraq using Long Ashton research station weather generator version 8 downscaled Coupled Model Intercomparison Project phase 6 climate scenarios

Zahraa Alaa Alsultani[1*], Rana Abd Al-Hadi Mukheef[2]

[1] Water Resources Engineering Department, College of Engineering, Al-Qasim Green University, 51013 Babylon, Iraq
[2] Civil Engineering Department, Collage of Engineering, Al-Qasim Green University, 51002 Babylon, Iraq
* Corresponding author email: zahraaalaa@wrec.uoqasim.edu.iq

ABSTRACT

Climate change poses significant challenges to arid and semi-arid regions, where rising temperatures and variable precipitation patterns exert increasing pressure on water resources. This study investigates future climate projections for southern Iraq, focusing on Basrah, Dhi Qar, and Al-Muthanna, using the LARS-WG8 stochastic weather generator driven by outputs from four CMIP6 global climate models under the SSP2-4.5 and SSP5-8.5 scenarios. Historical daily records (1995–2024) of precipitation, maximum temperature (Tmax), and minimum temperature (Tmin) were employed for model calibration and validation. The results indicate a consistent warming trend across the study area. Annual Tmax is projected to increase by approximately 3.1 °C under SSP2-4.5 and 4.6–4.9 °C under SSP5-8.5, while Tmin is expected to rise by 2.7–2.9 °C and 3.9–4.2 °C, respectively. This trend reflects a reduction in the diurnal temperature range and suggests intensified heat stress conditions. In parallel, projected annual precipitation exhibits a gradual decline, ranging from 3–6 mm in the near future to 5–10 mm in the far future. The combined effects of increasing temperatures and decreasing precipitation highlight the growing climate vulnerability of southern Iraq and emphasize the urgent need for effective adaptation strategies. These findings provide valuable insights for climate risk assessment and support sustainable water resource management in arid and semi-arid regions.

Keywords: climate change, temperature projection, precipitation projection, LARS-WG8, CMIP6, SSP scenarios.

INTRODUCTION

Climate change has emerged as a characteristic problem of the twenty-first century because it has reached across all spheres of the atmosphere, hydrological processes, and socioeconomic mechanisms of the planet (Spiridonov et al., 2025;Al-Maliki, 2025). The escalating levels of greenhouse gases are currently closely associated with the growing surface air temperatures, changes in the regimes of precipitation, and the growing frequency and intensity of climatic extremes, according to the Intergovernmental Panel on Climate Change (IPCC) (Allan et al., 2023; Forster et al., 2025). Such changes are especially sharp in arid and semi-arid areas, the climatic variability of which has a direct bearing on water resources, agriculture, human health, and ecosystem functioning (Xu and Yang, 2017; Alkandari et al., 2026). These observations are consistent with recent studies emphasizing that climate change has become a major obstacle to sustainable development in arid and semi-arid regions, where increasing temperatures and climate variability pose growing challenges for water resources, food security, and socioeconomic resilience (Alsufyani, 2025).

As one of the regions the most susceptible to the effects of climate change, the Middle East, and Iraq, in particular, is characterized by the overwhelmingly dry climate, great rates of evapotranspiration, and dependence on surface and groundwater resources with limited nature (Adamo et al., 2022; Al-Hussein et al., 2024; Riyadh et al., 2026). It can be seen in observational analysis and climate projections that the warming trend is persistent across Iraq, and the frequency of heatwaves and altered precipitation patterns put water security, agricultural productivity, and environmental sustainability at risk (Al-Naffakha et al., 2025; Shehab and Alsltany, 2025). As an example, the recent climate evaluations indicate that there is severe warming in both the mid and southern parts of Iraq with trends anticipated under different scenarios of emissions (Abdulhussein et al., 2024). In addition, localized research involving sophisticated climate models has pointed to the fact that the minimum and maximum temperatures will rise during the middle of this century, and the amount of precipitation is unpredictable as a result of the variability of models (Abdulsahib et al., 2024; Reyad and Fahad, 2025).

The impact of these shifts is not limited to the changes in temperature and precipitation trends but to more environmental and socioeconomic issues. The reduction in river flows, the rising number of droughts, and the escalation of water scarcity have already affected the agricultural production and the rural livelihood of people in Iraq (Eltaif et al., 2024). The findings are consistent with those of the research indicating that there were severe instances of climate-induced droughts in West Asia that would have been significantly less severe without the anthropogenic warming (Al-Ibady et al., 2026). These pressures make it imperative to have solid climate projections at scales that are pertinent to local decision-making. In addition to reliable climate projections, sustainable water resource management requires continuous assessment of water quality because climate variability may alter the physicochemical characteristics of aquatic systems and influence ecosystem functioning (Nyamweha et al., 2025).

Southern Iraq is highly vulnerable to the impacts of climate change, with Basrah, Dhi Qar, and Al-Muthanna representing key provinces characterized by critical wetland ecosystems, extensive agricultural landscapes, and rapidly expanding urban populations (Cornforth et al., 2022; Muhaimeed et al., 2025). These governorates are subject to significant environmental stress, including wetland degradation, desertification, and heightened sensitivity to climatic extremes. Previous studies employing downscaling approaches to assess future climate trends in southern Iraq have consistently reported rising temperatures; however, projections of precipitation remain uncertain, with both increasing and decreasing trends depending on the selected climate model and emission scenario (Hadi et al., 2024).

In order to overcome the problem of spatial differences between the coarse global climate model outputs and local climate effects, downscaling techniques, including stochastic weather generators, are commonly employed. Long Ashton research station weather generator (LARS-WG) has been already applied in several studies conducted in the area, revealing that they are able to reproduce the observed climatology and provide future predictions of the daily weather variables (Punyawansiri and Kwanyuen, 2020). As an example, the LARS-WG has been used to predict precipitation patterns in cities in Northern Iraq, which once again justifies its application in the evaluation of the impact of climate on the region (Abed et al., 2025).

Recent advances in climate modeling through the sixth phase of the Coupled Model Intercomparison Project (CMIP6) introduced the shared socioeconomic pathways (SSPs), which integrate socioeconomic development pathways with greenhouse gas emission trajectories, enabling more comprehensive assessments of future climate under different mitigation and adaptation scenarios. Building on these advances, this study employs the latest LARS-WG8 weather generator to downscale outputs from four state-of-the-art CMIP6 Global Climate Models (HadGEM, CanESM, BCC-CSM2-MR, and CMCC-Micro6) under SSP2-4.5 and SSP2-8.5. The model was calibrated and validated using observed daily precipitation, minimum temperature, and maximum temperature records for the baseline period (1995–2024). Future climate projections for 2025–2060 were analyzed over two climatological periods (2025–2042 and 2043–2060) using a multi-model ensemble approach to reduce projection uncertainty. The study provides high-resolution monthly and annual projections of temperature and precipitation for three climate-vulnerable governorates in southern Iraq, offering robust scientific information to support water-resource management, agricultural planning, environmental management, and climate adaptation strategies.

MATERIALS AND METHODS

Description of the study area

Iraq lies in arid to semi-arid Middle East, the hydrological system of which is characterized by a high evaporation of the land and the small amounts of precipitation per year. It is specifically in Southern Iraq, which is among the most heat-prone areas in the world, that the heat may sometimes reach over 45 °C during summer (Muslih and Abbas, 2025). The hottest period of the year is August, whereas the coldest month is January, with an average monthly temperature varying between 5 °C and 10 °C. The rainfall is mainly received during winter (October-May) and has a considerable interannual variability because of the regional climatic oscillations (Salman et al., 2019).

The present study focuses on three governorates in southern Iraq, Basrah, Dhi Qar, and Al-Muthanna, which represent some of the most climate-vulnerable and environmentally stressed regions in the country (Figure 1). These areas are characterized by high ecological sensitivity, persistent water scarcity, and a pronounced susceptibility to the long-term impacts of climate change (Nile et al., 2025).

Table 1 represents three meteorological stations that were sampled in each governorate to determine alterations in precipitation and temperature using projected climate conditions. The data of these stations will be of high quality in terms of daily observation documents in the year 1995-2024 which were utilized as reference data in calibration and validation of LARS-WG8 weather generator.

Observational climate data

Historical daily meteorological data, including precipitation (mm), minimum air temperature (Tmin, °C), and maximum air temperature (Tmax, °C), were obtained from the Iraqi Meteorological

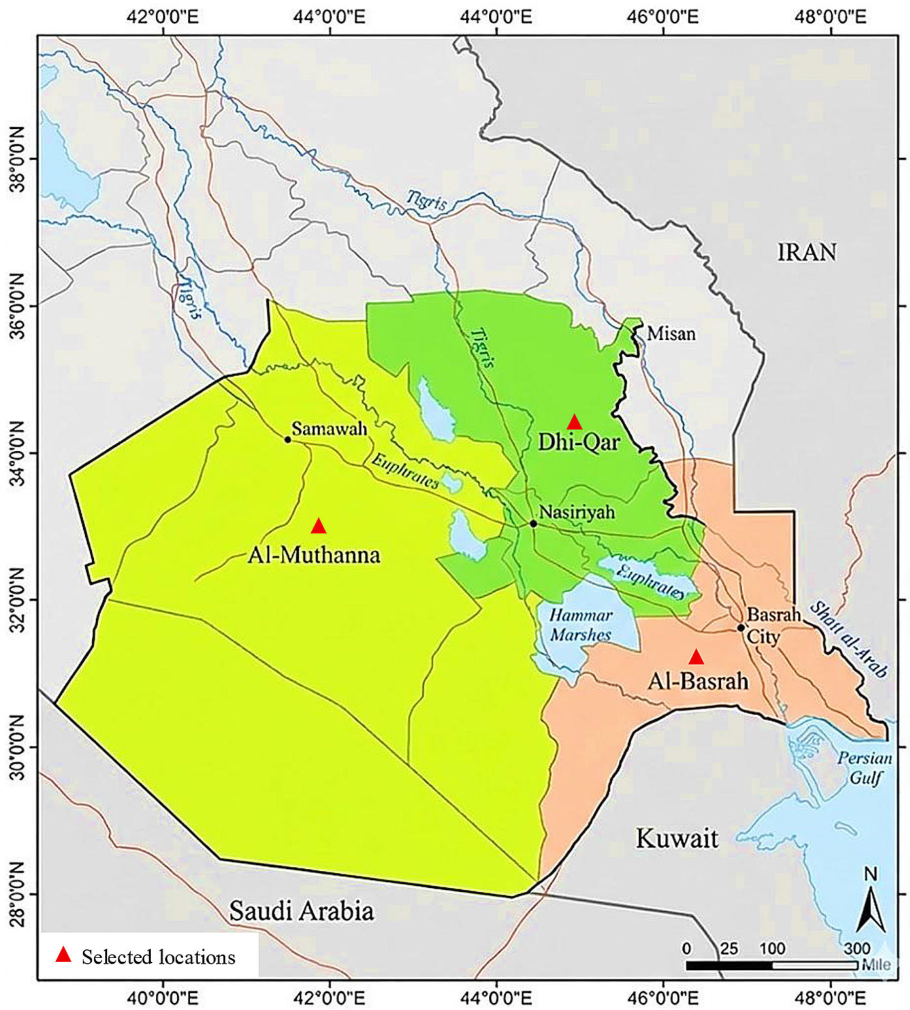

Figure 1. Distribution of the selected meteorological monitoring stations within the study region

Organization and Seismology (IMOS) for the Basrah, Dhi-Qar (Nasiriyah), and Al-Muthanna (Samawah) meteorological stations. The datasets cover the baseline period 1995–2024 and were acquired through an official data request to IMOS. The data were supplied in digital spreadsheet format (Microsoft Excel) as continuous daily records for each station.

Prior to their use in the LARS-WG8 weather generator, the observational data underwent comprehensive quality control and preprocessing to ensure accuracy, consistency, and completeness. The datasets were examined for missing values, duplicate records, inconsistencies in dates and measurement units, and temporal continuity. Short gaps (≤3 consecutive days) were filled using linear interpolation for temperature variables and nearest-neighbor temporal interpolation for precipitation, whereas longer gaps were reconstructed using data from the nearest meteorological station with similar climatic characteristics when available. Potential outliers were identified through statistical screening based on monthly climatological ranges, z-score analysis, and visual inspection of time-series data. Suspected anomalous values were verified against neighboring station records and retained only when consistent with regional meteorological conditions; otherwise, they were treated as missing values and reconstructed using the adopted gap-filling procedures. Records containing physically unrealistic measurements or prolonged missing periods that could not be reliably reconstructed were excluded from the analysis.

Following preprocessing, the final dataset provided a continuous and internally consistent 30-year daily climate record (1995–2024) suitable for calibrating and validating the LARS-WG8 model and for generating reliable downscaled climate projections. The observational datasets are subject to IMOS data-sharing regulations and are therefore not publicly available; however, they are available from the corresponding author upon reasonable request and, where required, with permission from IMOS.

Overview of the modeling framework

A combination of modeling was used to create high-resolution site-specific daily climate forecasts of southern Iraq. The method is a combination of past-based observations, stochastic weather modeling, global climate models, and emission scenarios to come up with a credible downscaled projection, as shown in Figure 2.

The model was calibrated and validated using historical daily records of precipitation, minimum temperature (Tmin), and maximum temperature (Tmax) obtained from meteorological stations. Based on these observations, there are correct methods of reproducing local climate patterns. This was then followed with analysis of the LARS-WG8 stochastic weather generator

Table 1. Geographic locations of the selected meteorological stations in southern Iraq and the length of their observational records

No.	Station	Latitude (N)	Longitude (E)	Altitude (m a.s.l.)	Record length
1	Basra	30° 31′ N	47° 48′ E	2	1995–2024
2	Dhi-Qar	31° 03′ N	46° 16′ E	5	1995–2024
3	Al-Muthanna	31° 19′ N	45° 17′ E	11	1995–2024

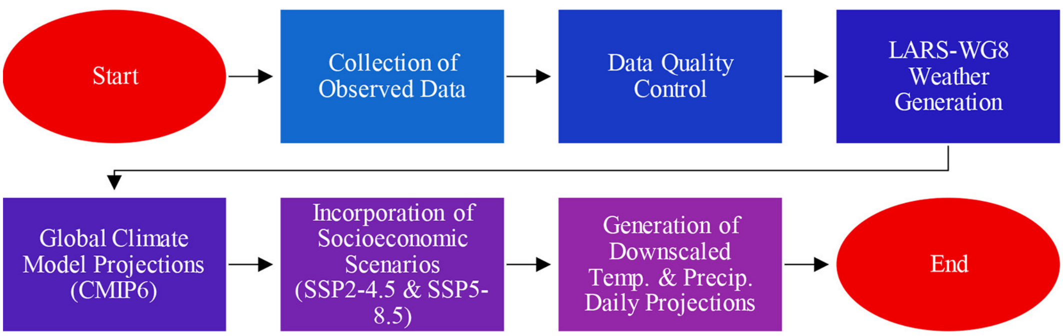

Figure 2. Conceptual framework for generating site-specific daily climate projections using observed data, LARS-WG8, CMIP6 GCMs, and SSP scenarios

to produce several synthetic climate sequences, maintaining the statistical distribution, and temporal correlation of the observed variables.

Four CMIP6 global climate models (HadGEM, CanESM, BCC-CSM2-MR and CMCC-Micro6) were used to obtain future climate projections. The uncertainty of each individual model was minimized by a multi-model ensemble approach which also produced an extensive spectrum of possible climate futures. The effect of the various greenhouse gas trajectories on the climate of the location was assessed by using two contrasting shared socioeconomic pathways (SSP2-4.5) and SSP5-8.5, which presented moderate mitigation and high emissions respectively.

Lastly, LARS-WG8 combined the outputs and SSP signals of the GCM models to generate downscaled climatic projections on a daily, site-specific basis (NASA, 2026). These estimates capture both local climatological features and global changes in climatic features, and they are a powerful instrument to determine future variations in temperature and precipitation in southern Iraq.

LARS-WG8 weather generator

The LARS-WG8 stochastic weather generator was configured using the default semi-empirical probability distributions implemented in the software to reproduce the statistical characteristics of daily precipitation, Tmin, and Tmax. Model calibration was performed independently for each meteorological station using the observed daily climate records for the baseline period (1995–2024). During calibration, LARS-WG8 automatically estimated the statistical parameters describing wet and dry spell distributions, daily precipitation occurrence and amounts, and the probability distributions of daily Tmin and Tmax for each month of the year.

Following successful calibration, the model generated synthetic daily weather series representing the baseline climate, which were compared with the observed records through statistical validation. Future climate projections were then produced by applying the CMIP6-derived climate change factors for each selected GCM and SSP scenario. For each station, 100 stochastic realizations were generated for every GCM–SSP combination, each having the same length as the corresponding projection period (18 years for 2025–2042 and 18 years for 2043–2060). Ensemble averages of the generated realizations were used in the subsequent analyses to minimize stochastic variability and improve the robustness of the projected climate signals.

The model was executed using the standard LARS-WG8 configuration without modification of the internal stochastic generation algorithms. Monthly statistics derived from the synthetic datasets were subsequently analyzed to evaluate projected changes in precipitation, maximum temperature, and minimum temperature under the selected climate scenarios.

The model that is used to determine the daily occurrence of precipitation is a two state Markov chain:

$$P_{ij} = \Pr(X_{t+1} = j \mid X_t = i), i, j \in \{0,1\} \quad (1)$$

where: X_t is the day's state (0 = dry, 1 = wet).

The amount of the precipitation and the temperature are produced through resampling of the empirical cumulative distribution functions (CDFs) and are correlated with the precipitation occurrence.

The model was calibrated using the records that were observed and tested on another independent subset. Table 2 provides an overview of performance indicators of statistical performance that have been applied to assess LARS-WG8 simulations.

Table 2. Statistical performance indicators for LARS-WG8 calibration and validation

Indicator	Description	Formula / Notes	Limitations
RMSE	Root mean square error	–	0 to +∞
MBE	Mean bias error	$\text{MBE} = \frac{1}{n}\sum_{i=1}^{n}(S_i - O_i)$	-∞ to +∞
R^2	Coefficient of determination	$R^2 = 1 - \frac{\sum(O_i - S_i)^2}{\sum(O_i - \bar{O})^2}$	0 to 1
KS test	Kolmogorov–Smirnov test	Assesses similarity between observed and simulated distributions	0 to 1

Global climate models (CMIP6)

In the present study, four CMIP6 global climate models (GCMs) were employed to generate robust projections of future climate conditions in southern Iraq. These models were selected for their capability to effectively simulate key climatic processes in arid and semi-arid regions, including temperature variability, precipitation extremes, and seasonal distribution patterns. To reduce uncertainties associated with individual models, a multi-model ensemble approach was adopted, providing a more reliable assessment of future climate trends. The characteristics of the selected models are summarized in Table 3.

Emission and socioeconomic scenarios

To determine the future climate conditions, two Shared Socioeconomic Pathways (SSPs) were taken into consideration with the opposite trajectories of greenhouse gas emissions and radiative forcing. These situations offer an opportunity to consider intermediate and high-risk southern Iraq climate future. Radiative forcing (ΔF) drives the projections of the selected GCMs and is defined as:

$$\Delta F = F_t - F_0 \quad (2)$$

where: F_t is the radiative forcing at time t and F_0 is the pre-industrial baseline. The two scenarios used in this study are summarized in Table 4.

Time-period definition

Three periods of time were used in the study to compare the past climatic conditions and future projections in southern Iraq. These intervals allow the evaluation of the performance of calibration as well as climate trends within a near- and far-term period. The weather generator is calibrated and validated using the baseline period (1995–2024). The near-future period (2025–2042) entails the early signals of climate change, and the far-future period (2043–2060) enables the analysis of the medium-term trends and possible consequences. Table 5 summarizes the information about the time periods that were employed in this study.

Model calibration and validation

The LARS-WG8 weather generator was calibrated by modifying the model parameters to reduce the difference between measured (O_i) and simulated (S_i) climatic variables of daily variation. Independent subset of the observations was used in validation. The root mean square error (RMSE), mean bias error (MBE), coefficient of determination (R^2) and Kolmogorov-Smirnov (KS) test of similarity of distributions were used as tools to assess model performance.

Findings verified that LARS-WG8 is a reliable reproducer of both precipitation and temperature patterns, such as local variability and extremes. This guarantees that the downscaled climate projections capture the future climate behavior in the selected SSP scenarios, which will serve as a solid basis to future impact assessment.

To ensure the reproducibility of the proposed methodology, the complete workflow adopted in this study is summarized in Figure 3.

RESULTS AND DISCUSSION

Model validation

The workability of the LARS-WG8 weather generator was examined by evaluating the results

Table 3. Characteristics of the selected CMIP6 global climate models used in this study for southern Iraq projections

Model	Institution	Resolution	Key Features	Relevance	Ref.
HadGEM	UK Met Office	0.83° × 0.56°	High-resolution mid-latitude simulation	Captures temperature and rainfall variability	Guarino et al., (2020)
CanESM	Canadian Centre for Climate Modelling	2.81° × 2.79°	Advanced carbon cycle and climate feedback	Reliable projection of temperature extremes	Swart et al. (2019)
BCC-CSM2-MR	Beijing Climate Center	1.1° × 1.1°	Regional monsoon variability and precipitation extremes	Represents wet/dry spells in arid/semi-arid regions	Wu et al. (2020)
CMCC-Micro6	CMCC, Italy	0.75° × 0.75°	Mediterranean and Middle East climate representation	Captures local seasonal climate patterns	Cherchi et al. (2019)

Table 4. Characteristics of the selected shared socioeconomic pathways (SSPs) used for climate projections in southern Iraq

Scenario	Radiative forcing (W/m²)	Emissions	Relevance
SSP2-4.5	4.5	Moderate mitigation	Intermediate climate change scenario
SSP5-8.5	8.5	High emissions	High-risk, strong warming scenario

Table 5. Definition of baseline, near-future, and far-future periods for calibration and climate projection analysis

Period	Years	Purpose
Baseline	1995–2024	Calibration and validation
Near-future (NF)	2025–2042	Early climate change assessment
Far-future (FF)	2043–2060	Medium-term trend analysis

of the 1995–2024 historical climate data before using the outcomes to analyze future climate projections. Model validation was conducted using daily precipitation, Tmin, and Tmax data collected from three meteorological stations in southern Iraq, namely Basrah, Dhi Qar, and Al-Muthanna.

As can be seen in Table 6, the model showed a very good correlation with the monitored data. The coefficient of determination (R^2) values ranged from 0.87 to 0.95 for precipitation and 0.92 to 0.95 for temperature, indicating that LARS-WG8 successfully captures both the magnitude and temporal variability of observed climate variables. The RMSE values were relatively low, with precipitation errors between 2.3 and 2.5 mm and temperature errors between 0.8 and 1.1 °C, further confirming the accuracy of simulated daily values. MBE values were minimal, ranging from -0.12 to 0.15, reflecting negligible systematic over- or underestimation by the model. Additionally, Kolmogorov-Smirnov (KS) test p-values were consistently

Figure 3. Overall workflow of the climate downscaling and projection methodology adopted in this study

above 0.75, indicating strong agreement between the observed and simulated distributions for all variables.

Table 6 summarizes the projected annual average Tmax, Tmin, and total precipitation for the three meteorological stations (Basrah, Dhi-Qar, and Al-Muthanna) under the baseline period (1995–2024) and the two future periods, namely the Near Future (2025–2042) and Far Future (2043–2060), based on the SSP2-4.5 and SSP2-8.5 climate scenarios. The table provides an integrated overview of the expected long-term changes in the regional climate, facilitating comparison among stations, future periods, and emission pathways while highlighting the projected warming trend and changes in annual precipitation across southern Iraq.

Taken together, these findings (Table 7) suggest that LARS-WG8 is very effective in reproduction of statistical properties of historical daily climate in southern Iraq. The high validation of the model on various metrics gives the assurance that the model can be used to reliably produce downscaled CMIP6 climate simulations that can be used to undertake in-depth evaluations of future temperature and precipitation variability in the SSP2-4.5 and SSP5-8.5 scenarios.

Temperature projections

The estimated monthly temperatures of Basrah, Dhi-Qar, and Al-Muthanna in Figures 4 and 5 show that all months show a strong and consistent increasing trend of temperatures compared to the

Table 6. Seasonal and annual average temperatures and total precipitation

Station	Period	Scenario	Annual Tmax (°C)	Annual Tmin (°C)	Annual precipitation (mm)
Basrah	Baseline (1995–2024)	–	32.3	19.4	125
	Near Future (2025–2042)	SSP2-4.5	33.8	20.5	120.1
		SSP2-8.5	34.6	21.3	121.8
	Far Future (2043–2060)	SSP2-4.5	35.2	22.1	117
		SSP2-8.5	36.9	23.5	119.4
Dhi-Qar	Baseline (1995–2024)	–	31.9	18.9	133.1
	Near Future (2025–2042)	SSP2-4.5	33.5	20.3	127.2
		SSP2-8.5	34.5	21.1	128.7
	Far Future (2043–2060)	SSP2-4.5	35	21.6	123.2
		SSP2-8.5	36.7	22.9	125.1
Al-Muthanna	Baseline (1995–2024)	–	31.5	18.1	125
	Near Future (2025–2042)	SSP2-4.5	33.1	19.4	119.9
		SSP2-8.5	34.1	20.2	121.4
	Far Future (2043–2060)	SSP2-4.5	34.7	20.8	116.3
		SSP2-8.5	36.3	22.1	118.5

Table 7. Statistical performance indicators for LARS-WG8 calibration and validation (1995-2024) across three southern Iraq stations

Station	Variable	R^2	RMSE	MBE	KS Statistic	p-value
Basrah	Precipitation	0.89	2.3 mm	0.12 mm	0.21	0.78
	Tmin	0.95	0.8 °C	-0.10 °C	0.18	0.82
	Tmax	0.94	1.0 °C	0.05 °C	0.19	0.79
Dhi-Qar	Precipitation	0.87	2.5 mm	0.15 mm	0.25	0.75
	Tmin	0.93	0.9 °C	-0.12 °C	0.2	0.8
	Tmax	0.92	1.1 °C	0.08 °C	0.22	0.77
Al Muthanna	Precipitation	0.88	2.4 mm	0.14 mm	0.24	0.76
	Tmin	0.94	0.8 °C	-0.09 °C	0.19	0.81
	Tmax	0.93	1.0 °C	0.07 °C	0.2	0.78

baseline period (1995–2024). Across all stations, both maximum (Tmax) and minimum (Tmin) temperatures increase under SSP2-4.5 and SSP5-8.5, with warming intensifying from the near-future (2025–2042) to the mid-future (2043–2060) and being more pronounced under the high-emission SSP5-8.5 scenario.

Winter warming is moderate but meaningful, with January Tmax rising by 2–3.5 °C and Tmin by 2–4 °C under SSP5-8.5 by 2060, reflecting reduced cold-season variability. The most substantial warming occurs during summer months: July and August Tmax frequently exceed 50 °C under SSP5-8.5 in the mid-future, while Tmin reaches 35–36.6 °C, indicating extreme heat stress and limited nighttime cooling. Spring and autumn months also warm significantly, with Tmax increases of 3–4 °C, effectively extending the duration of hot conditions and shortening thermally comfortable periods.

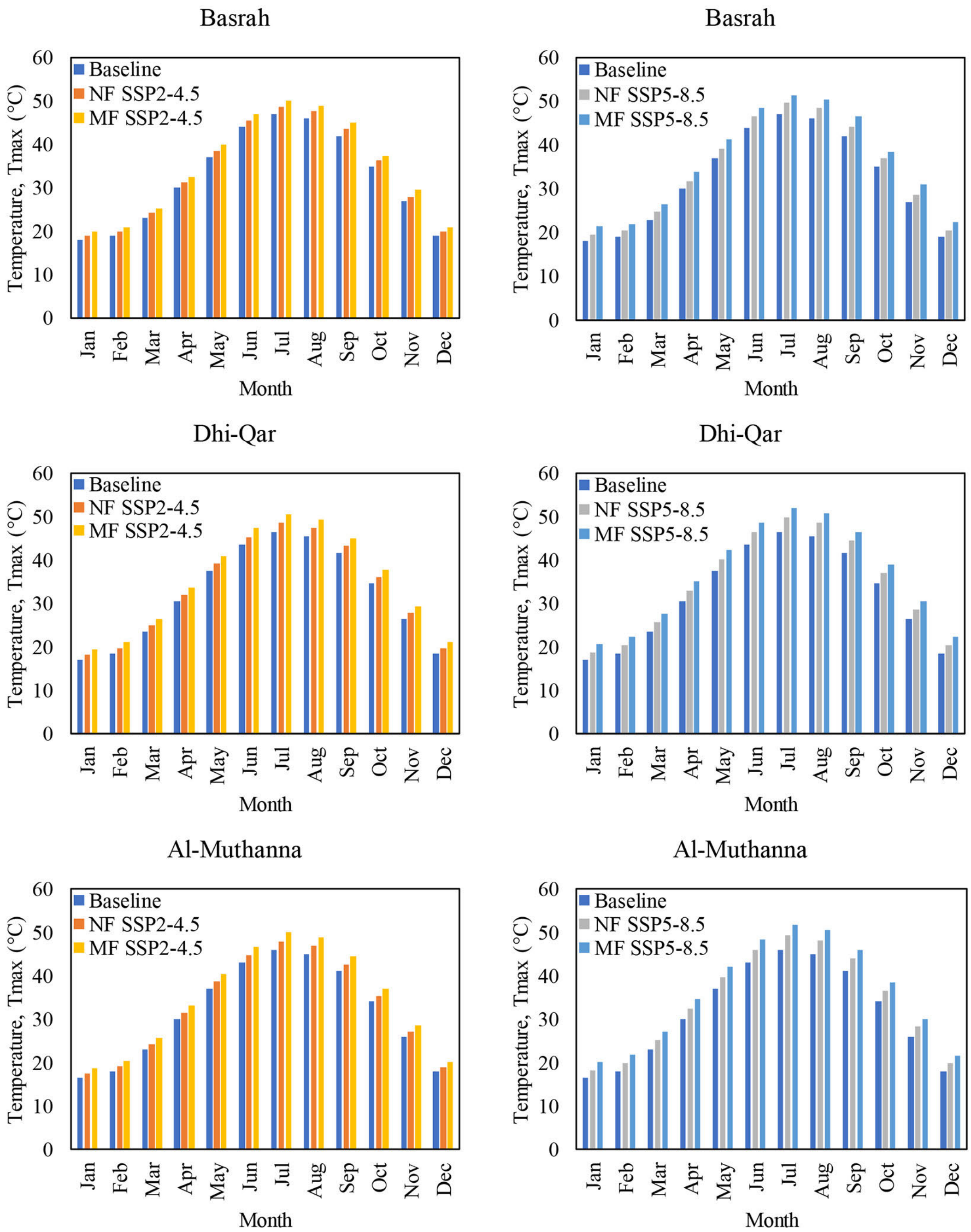

Figure 4. Comparison of observed average monthly maximum temperatures for the baseline period (1995–2024) with projected changes under SSP2-4.5 and SSP5-8.5 scenarios for the near future (2025–2042) and far future (2043–2060)

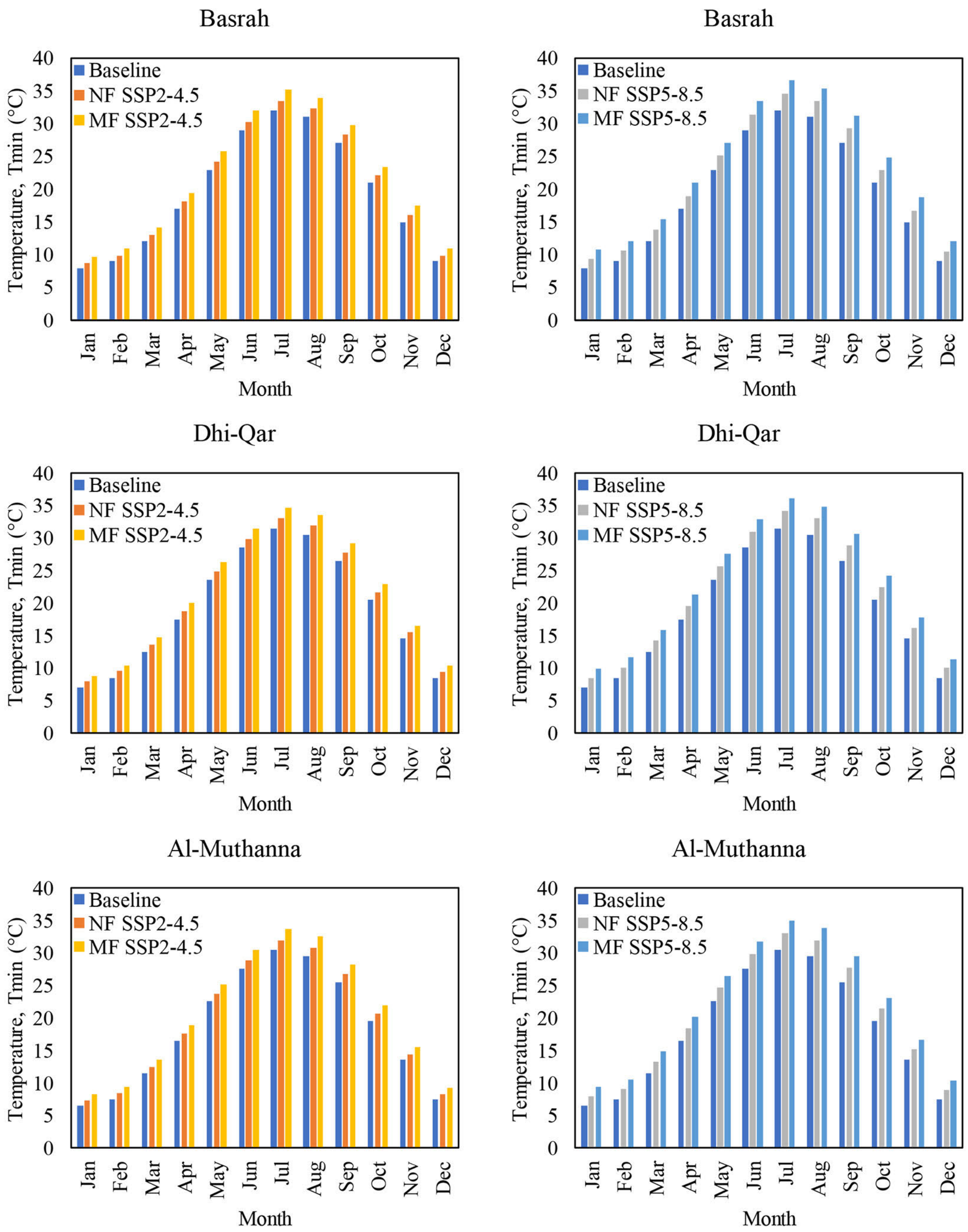

Figure 5. Comparison of observed average monthly minimum temperatures for the baseline period (1995–2024) with projected changes under SSP2-4.5 and SSP5-8.5 scenarios for the near future (2025–2042) and far future (2043–2060)

In all stations, the increase in Tmin is, on average, greater than the increase in Tmax resulting to a decreased diurnal range of temperatures, which might increase the nocturnal heat stress, the cooling energy demand, and evapotranspiration. The difference between SSP2-4.5 and SSP5-8.5 is greater in the far-future which indicates the sensitivity of the southern Iraq thermal regime to emission pathways and the importance of mitigation.

On the whole, the findings show that more frequent and severe heat extremes, extended hot seasons, and high nighttime temperatures are likely in southern Iraq, and this threat is great to the water resources, agriculture, and human health, as well as infrastructure (Alsultani et al., 2025). Such forecasts highlight the importance of considering climate adjustment and mitigation measures of heat risks when planning regions, especially in cases of high emission levels.

Annual temperature changes

The projected annual temperature changes for the three stations (Figures 6 and 7) indicate a consistent warming trend across all CMIP6 models and scenarios. Both maximum and minimum temperatures increase relative to the baseline period (1995–2024), with stronger warming observed under SSP5-8.5 and in the far-future period (2043–2060).

At Basrah, annual Tmax increases range from 1.5–1.8 °C in the near-future under SSP2-4.5 to 4.1–4.6 °C in the far-future under SSP5-8.5. Corresponding Tmin increases are slightly lower but still substantial, ranging from 1.2–1.5 °C in the near-future to 3.4–3.9 °C in the far-future. These projections indicate that Basrah will experience intensifying heat extremes and warmer nights, which may amplify heat stress and water demand.

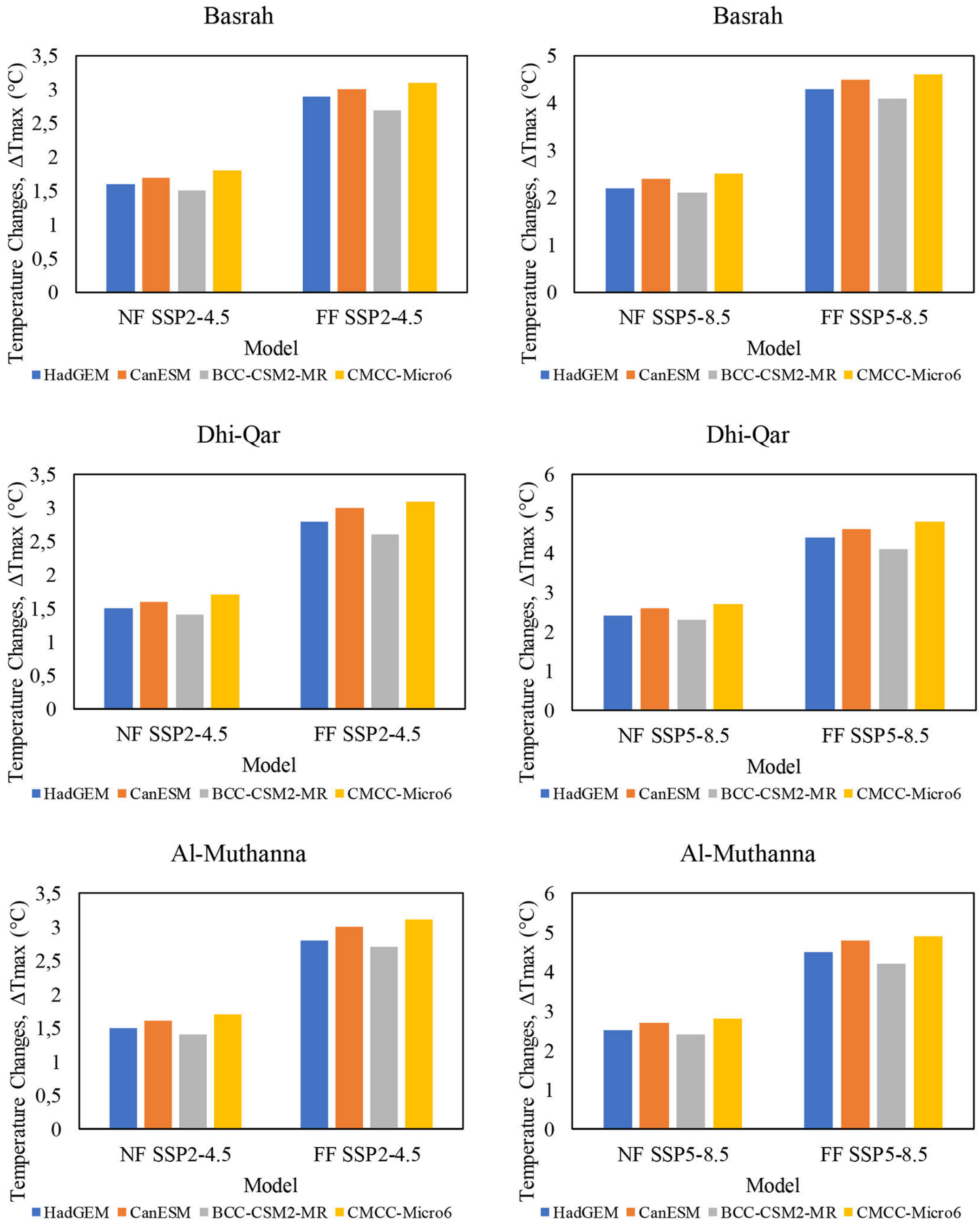

Figure 6. Differences in projected annual maximum temperatures at all stations for the two near and far future periods relative to the baseline (1995–2024), under SSP2-4.5 and SSP5-8.5, using four selected CMIP6 global climate models

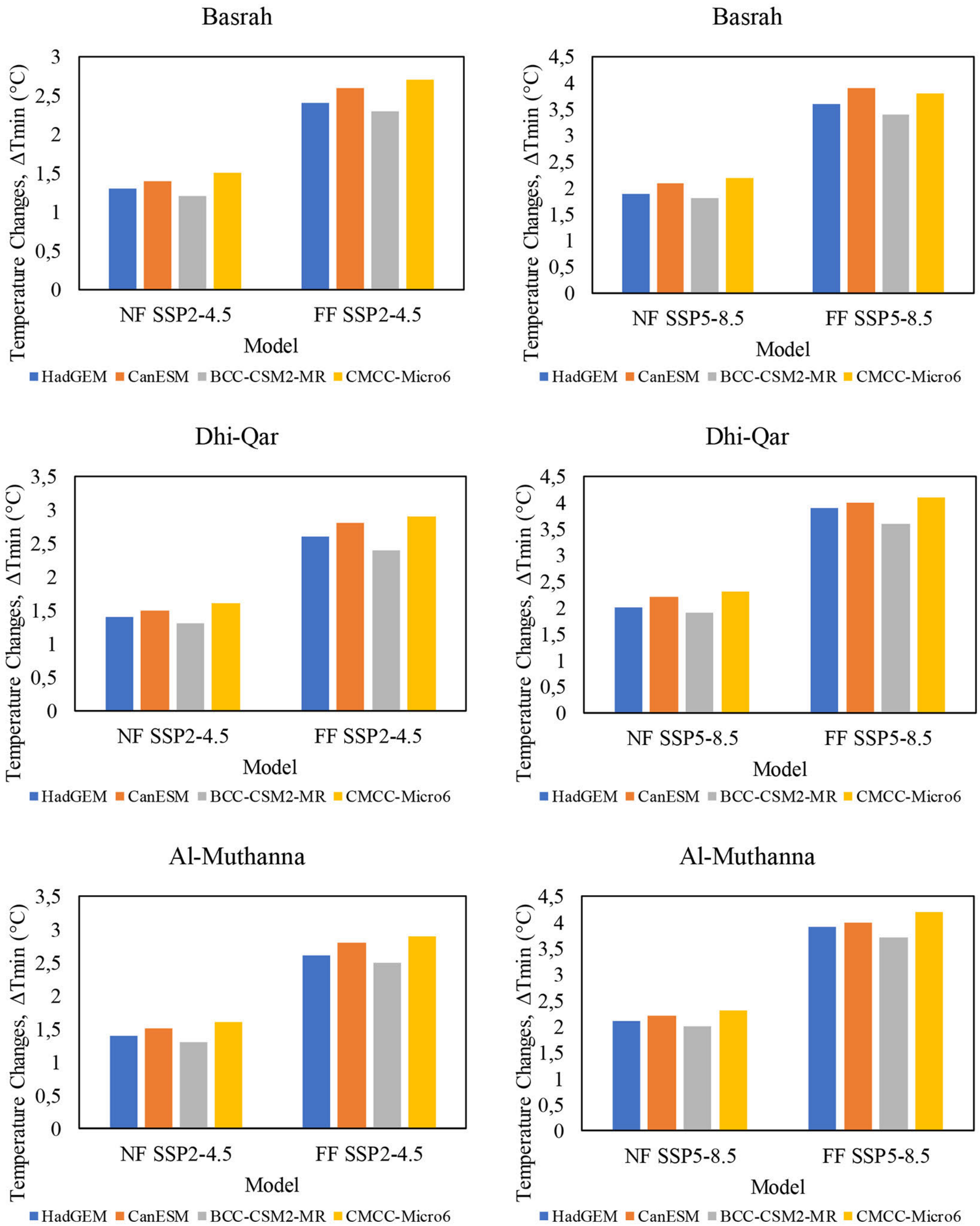

Figure 7. Differences in projected annual minimum temperatures at all stations for the two near and far future periods relative to the baseline (1995–2024), under SSP2-4.5 and SSP5-8.5, using four selected CMIP6 global climate models

For Dhi-Qar, Tmax increases are slightly lower in the near-future (1.4–1.7 °C) and rise to 4.1–4.8 °C in the far-future under SSP5-8.5. Tmin follows a similar pattern, increasing from 1.3–1.6 °C in the near-future to 3.6–4.1 °C by the mid-future. This pattern reinforces the expectation of intensified summer heat and warmer winters, potentially impacting agriculture and human health.

In Al-Muthanna, Tmax projections are comparable to those of Basrah and Dhi-Qar, with far-future SSP5-8.5 increases up to 4.9 °C, while Tmin rises up to 4.2 °C. Across all stations, Tmin increases slightly exceed or closely match Tmax changes, indicating a reduced diurnal temperature range, which is consistent with regional warming patterns driven by greenhouse gas forcing.

The multi-model ensemble approach shows good agreement among the four CMIP6 GCMs (HadGEM, CanESM, BCC-CSM2-MR, CMCC-Micro6), with differences of less than ±0.3 °C in most cases. This strengthens confidence in the robustness of the projected warming trends.

Generally, the findings indicate, there is a high level of climate stress in southern Iraq especially in SSP5-8.5 during far future, so that it affects the heatwaves, scarcity of water, energy demands and human health. The results highlight the need to embed mitigation and adaptation strategies to minimize susceptibility to increasing temperatures along these extremely climate-sensitive areas.

Figure 8 shows the estimates of the growth of annual maximum (Tmax) and minimum (Tmin) temperatures of the three southern Iraq stations under SSP2-4.5, and SSP5-8.5. The trend of warming is evident across all stations with the greatest increase under SSP5-8.5 during the distant future. Tmax is projected to rise by 3.1 °C under SSP2-4.5 and 4.6–4.9 °C under SSP5-8.5, with Al-Muthanna experiencing the highest increases, indicating heightened summer heat extremes. Tmin increases range from 2.7–2.9 °C under SSP2-4.5 and 3.9–4.2 °C under SSP5-8.5, slightly reducing the diurnal temperature range and limiting nighttime cooling. These scenarios imply aggravated heat stress to the populations, agriculture, and energy systems. In general, the findings identify the acceleration of warming in southern Iraq, more specifically in a high-emission scenario, the experiment showing the acute necessity to develop climate adaptation and mitigation strategies.

Precipitation patterns

The projected monthly precipitation of Basrah, Dhi-Qar and Al-Muthannah, in both SSP2-4.5 and SSP5-8.5 as illustrated in Figure 9 portrays, shows that both near future (2025–2042) and far-future (2043–2060) projects of the projected rainfall decline in most months. The most significant reductions can be seen in winter and early spring months that are crucial to the water resources. As an example, the January rainfall in Basrah is expected to decrease at a level of 26.9 mm (far-future) with SSP5-8.5 compared to 28.4 mm (baseline), and the same is the case with Dhi-Qar and Al-Muthanna. March also indicates slight reductions, which is an indicator of possible pressure on groundwater recharge and irrigation.

Summer months remain essentially rain-free, consistent with historical arid conditions, while transitional months (April-May and October-November) experience slight reductions (e.g., Basrah April precipitation decreases from 6.8 mm to 6.3–6.4 mm). Such minor but regular declines in effect decrease the duration of the wet season and decrease the time frame of water availability.

The scenario of SSP5-8.5 demonstrates a slight increase in declines in comparison to SSP2-4.5 with more intense reductions in the far-future showing that increasing emission pathways amplify regional drying trends. In general, warming and declining rainfall explain the potential effects of increasing water shortage, high evapotranspiration, and agriculture, water supply, and ecosystem services in southern Iraq. The mitigation of these new risks will require adaptation strategies including water storage, efficient irrigation and drought resistant crops.

Figure 10 illustrates the projected annual precipitation for Basrah, Dhi Qar, and Al-Muthanna, revealing a consistent decline across all four CMIP6 models under both SSP2-4.5 and

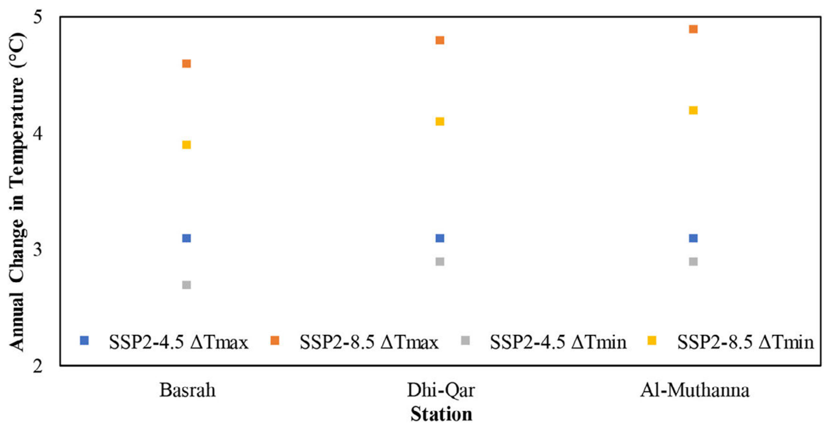

Figure 8. Projected variations in annual maximum and minimum air temperatures at the Basrah, Dhi-Qar, and Al-Muthanna meteorological stations under the selected climate scenarios

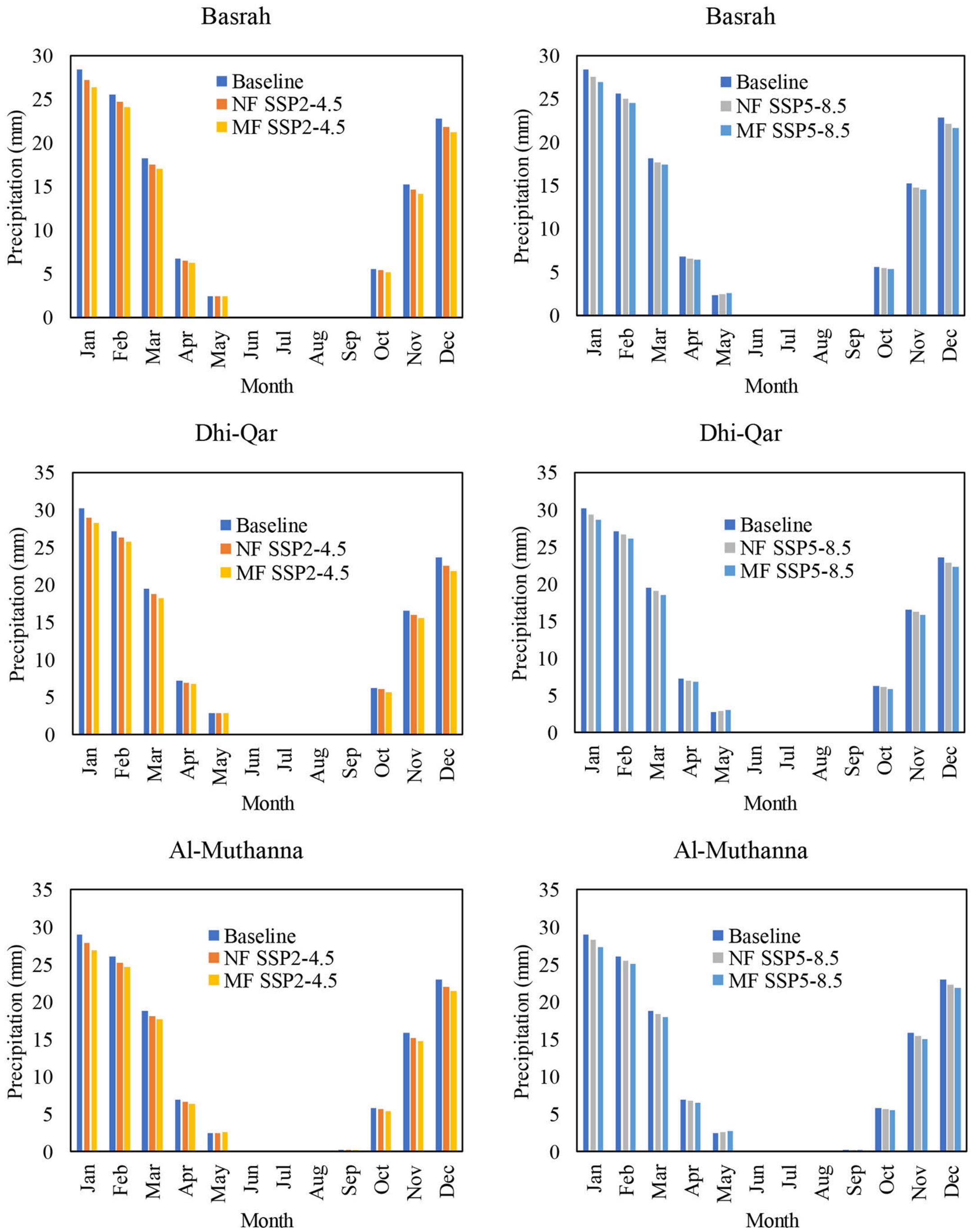

Figure 9. Monthly precipitation for baseline means (1995–2024) plus the projected changes under SSP2-4.5 and SSP5-8.5 for Near-Future (2025–2042) and Far-Future (2043–2060)

SSP5-8.5 scenarios. The reduction is more pronounced under the high-emission SSP5-8.5 scenario, particularly when comparing the near-future (2025–2042) with the far-future period (2043–2060). In the near future, precipitation is projected to decrease by approximately 3–6 mm, while a more substantial reduction of 5–10 mm is expected in the far future. The most significant decline is observed at Al-Muthanna, where reductions range between 7 and 9.5 mm.

This drying tendency is strongly predicted by the multi-model ensemble although there is some inter-model variability caused by varying sensitivity of regional precipitation and convective parameterization. The gradual decrease in precipitation, coupled with the increase in temperature, indicates the fact that there is growing climate stress in southern Iraq, which underlines the importance of adaptive strategies that include better water management,

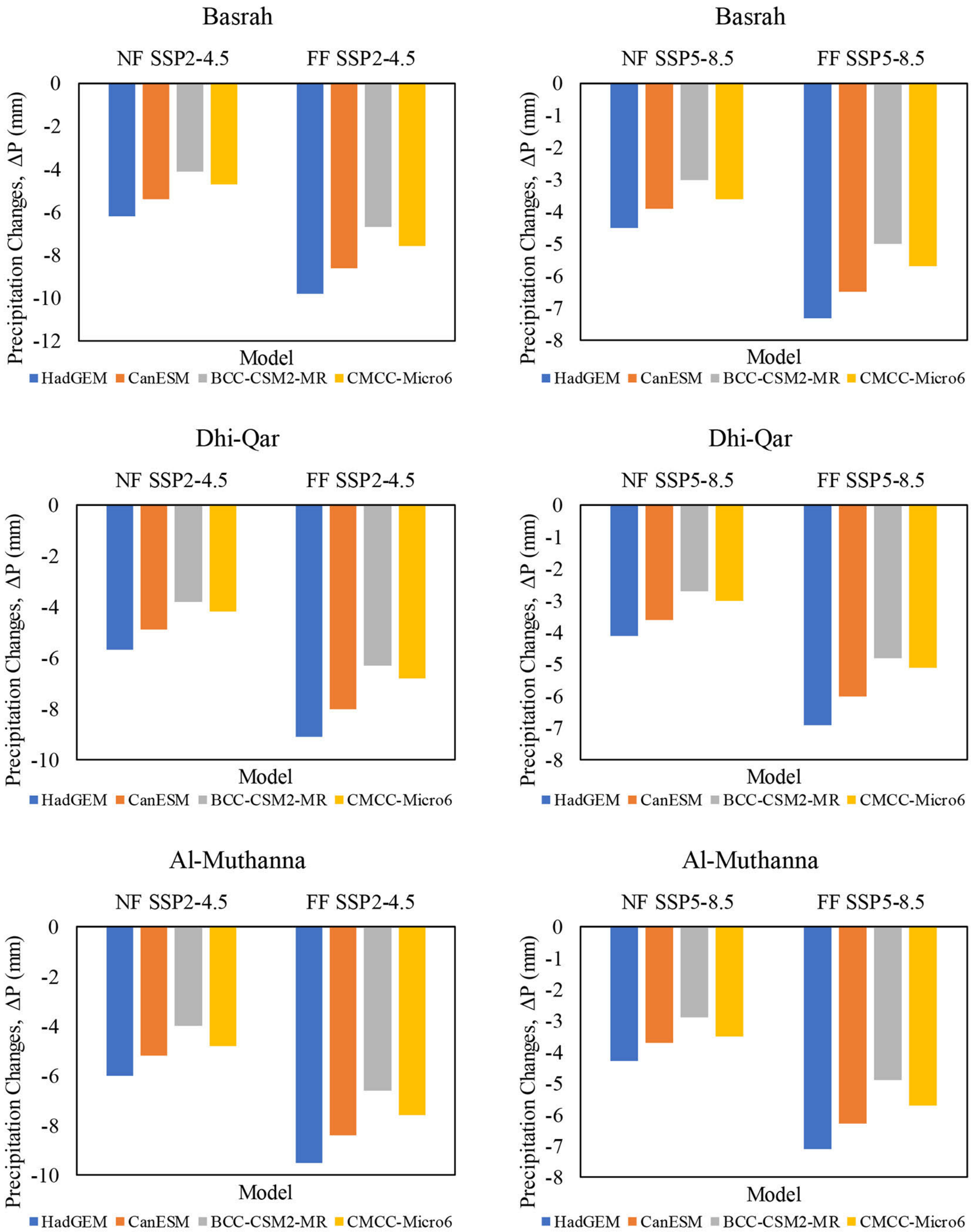

Figure 10. Differences in projected annual precipitation (ΔP, mm) relative to baseline (1995–2024)

harvesting of rainwater, and the use of drought-resistant agriculture.

The projected climate changes are consistent with previous studies conducted in Iraq and the Middle East, which consistently report increasing air temperatures and a general decline in precipitation under future climate scenarios. The projected warming across Basrah, Dhi-Qar, and Al-Muthanna, particularly under SSP2-8.5, agrees with recent CMIP6-based assessments indicating intensified summer heat and increasing climate stress in arid and semi-arid regions (IPCC, 2023; Almazroui et al., 2021; Salman et al., 2022). Likewise, the projected reduction in precipitation supports earlier findings that southern Iraq is likely to experience increasing water scarcity, although precipitation projections remain more uncertain because of differences among GCMs and downscaling methods (Chen et al., 2020; Almazroui et al., 2021). Overall, the agreement with previous studies enhances confidence in the projected warming trends, while highlighting the need for cautious interpretation of future precipitation changes.

The results also demonstrate the increasing vulnerability of southern Iraq to climate change. Future climate adaptation strategies should incorporate continuous environmental monitoring technologies capable of providing real-time information on environmental conditions and water resources, thereby enabling timely responses to climate-related risks and enhancing the effectiveness of adaptation measures (Oladosu et al., 2026). Furthermore, integrating high-resolution climate projections with environmental risk assessment frameworks can strengthen decision-making processes, improve vulnerability assessments, and support sustainable regional planning under future climate scenarios (Onambele et al., 2025). These approaches will contribute to more resilient water-resource management, agricultural planning, and climate adaptation in southern Iraq.

CONCLUSIONS

This study presents downscaled projections of daily climate variables for southern Iraq using the LARS-WG8 stochastic weather generator combined with four CMIP6 General Circulation Models under SSP2-4.5 and SSP5-8.5 scenarios. The main conclusion can be summarized as:

1. The results indicate a clear and consistent warming trend across Basrah, Dhi-Qar, and Al-Muthanna. Annual maximum temperatures (Tmax) are projected to increase by approximately 3.1 °C under SSP2-4.5 and 4.6–4.9 °C under SSP5-8.5, while minimum temperatures (Tmin) are expected to rise by 2.7–2.9 °C and 3.9–4.2 °C, respectively.
2. The reduction in the diurnal temperature range, particularly under high-emission scenarios, suggests elevated nighttime temperatures, which may intensify heat stress on populations, agriculture, and energy systems.
3. The projected precipitation results indicate a consistent decline across all stations and scenarios, with more pronounced reductions under SSP5-8.5, especially in the far-future period.
4. Annual precipitation is expected to decrease by approximately 3–6 mm in the near future and 5–10 mm in the far future, reflecting a cumulative drying trend.
5. The multi-model ensemble consistently captures this pattern, highlighting increasing vulnerability of water resources, soil moisture, and agricultural productivity in southern Iraq.

Overall, the combined impacts of increasing temperatures and decreasing precipitation emphasize the urgent need for targeted adaptation and mitigation strategies. These should include improved water resource management, the adoption of drought-resistant agricultural practices, and climate-resilient infrastructure planning to reduce risks and enhance the resilience of communities in this highly vulnerable region.

The observational climate data used in this study were obtained from the Iraqi Meteorological Organization and Seismology (IMOS) and are subject to institutional data-sharing policies.

REFERENCES

1. Abdulhussein, H. K., Al-Lami, A. M., Hashim, B. M. (2024). Air temperature projections over the mid and southern of Iraq during the 21th century under representative concentration pathways (RCPs), RCP 4.5 and RCP 8.5 scenarios. *The Iraqi Geological Journal*, 235-254.
2. Abdulsahib, S. M., Zubaidi, S. L., Almamalachy, Y., Dulaimi, A. (2024). Temperature and precipitation change assessment in the north of Iraq using LARS-WG and CMIP6 models. *Water, 16*(19), 2869.
3. Abed, T., Zubaidi, S., Almamalachy, Y., Abdellatif, M. (2025). Precipitation projection using LARS-WG and CMIP6 models. *Wasit Journal of Engineering Sciences*, *13*(4), 1–5.
4. Adamo, N., Al-Ansari, N., Sissakian, V., Jehad Fahmi, K., Ali Abed, S. (2022). Climate change: Droughts and increasing desertification in the Middle East, with special reference to Iraq. *Engineering, 14*(7), 235–273.
5. Al-Hussein, A. A., Hamed, Y., Al-Ozeer, A. Z., Gentilucci, M., Bouri, S. (2024). Impact of climatic changes on surface water in Middle East, Northern Iraq. *Environmental Earth Sciences, 83*(2), 48.
6. Al-Ibady, Q. A. N. A. K. (2026). Environmental changes and water scarcity and their impact on sustainable development in Iraq: A review. *Journal of Genetic and Environment Conservation, 14*(1), 1–12.
7. Alkandari, A. J., Alsayegh, M. A., Abdulraheem, A. A. (2026). Climate Change-Induced Variation in Ecosystem Structure in Arid Lands Countries. In *Fostering Arid Lands Agriculture in the Face of Climate Change: Mitigation and Adaptation Synergy* (pp. 339–367). Cham: Springer Nature Switzerland.
8. Allan, R. P., Arias, P. A., Berger, S., Canadell, J. G., Cassou, C., Chen, D.,..., Zickfeld, K. (2023). Intergovernmental panel on climate change (IPCC). Summary for policymakers. In *Climate change*

2021: The physical science basis. Contribution of working group I to the sixth assessment report of the intergovernmental panel on climate change (pp. 3–32). Cambridge University Press.

9. Al-Maliki, L. A., Mukheef, R. A. A. H., El-Tawil, K., Al-Ansari, N. (2025). Climate change trends and adaptation strategies in Southern Regions of Iraq. *Journal of Groundwater Science and Engineering, 13*(4), 449–468. doi:10.26599/JGSE.2025.9280065
10. Almazroui, M., Ashfaq, M., Islam, M. N., Rashid, I. U., Kamil, S., Abid, M. A.,..., Sylla, M. B. (2021). Assessment of CMIP6 performance and projected temperature and precipitation changes over South America. *Earth Systems and Environment, 5*(2), 155–183.
11. Al-Naffakha, J. T., Al-Qassabanda, M. R., Jafar, I. (2025). Decoding climate change: A comprehensive statistical insight into temperature anomalies in Iraq and its neighboring countries. *Al-Esraa University College Journal for Engineering Sciences, 7*(12), 36–48.
12. Alsufyani, A. (2025). Sustainability of alternative energy in Yemen: A comprehensive review. *Environmental Engineering, 3*(4), 23–39.
13. Alsultani, R., Abdulwahd, A. K., Hasan, A. R., Afan, H. A. (2025). A tiered hybrid life cycle assessment for sustainable water resources management in Iraq. *Civil and Environmental Engineering, 21*(2), 1348–1360.
14. Cherchi, A., Fogli, P. G., Lovato, T., Peano, D., Iovino, D., Gualdi, S.,..., Navarra, A. (2019). Global mean climate and main patterns of variability in the CMCC-CM2 coupled model. *Journal of Advances in Modeling Earth Systems, 11*(1), 185–209.
15. Cornforth, R., Saggioro, E., Petty, C., Pope, H., Tarnavsky, E. (2022). *Climate risk assessment for Iraq: The Southern Marshes eco-region and Persian Gulf and Shatt Al-Arab eco-region.* Walker Institute.
16. Eltaif, N. I., Gharaibeh, M. A., Fadhil Al-Quraishi, A. M. (2024). Impact of climate change on Iraq: severe water scarcity and desertification. In *Climate Change and Environmental Degradation in the MENA Region* (pp. 279-303). Cham: Springer Nature Switzerland.
17. Forster, P. M., Smith, C., Walsh, T., Lamb, W. F., Lamboll, R., Cassou, C.,..., Zhai, P. (2025). *Indicators of Global Climate Change–2024 Annual Update| Klean Insights*. Indicators.
18. Guarino, M. V., Sime, L. C., Schroeder, D., Lister, G. M., Hatcher, R. (2020). Machine dependence and reproducibility for coupled climate simulations: the HadGEM3-GC3. 1 CMIP Preindustrial simulation. *Geoscientific Model Development, 13*(1), 139-154.
19. Hadi, S. H., Alwan, H. H., Al-Mohammed, F. M. (2024). Analysis of climate change scenarios using the LARS-WG 8 model based on precipitation and temperature trends. *Civil Engineering Journal, 10*(12), 4019–4042.
20. Muhaimeed, A. S., Nassar, M. S., Katalan, B. A. (2025). The threat of climate change to vegetation health and land degradation in Iraq's diverse climatic environment. *American Journal of Agriculture and Forestry.*
21. Muslih, K. D., Abbas, A. M. (2024). Climate of Iraq. In *The geography of Iraq* (pp. 19–47). Cham: Springer Nature Switzerland.
22. NASA Earth Science Data. (2026). Global daily temperature and precipitation data. NASA Earthdata. Retrieved from https://earthdata.nasa.gov
23. Nile, B. K., Al-Saadi, R. J. M., Abdulameer, L., Al Maimuri, N. M., Al-Dujaili, A. N. (2025). Climate change impacts on river hydraulics: a global synthesis of hydrological shifts, ecological consequences, and adaptive strategies. *Water Conservation Science and Engineering, 10*(2), 48.
24. Nyamweha, B. R., Muhangi, C., Sunday, R., Muganyizi, D., Sserwadda, M., Tumwesigye, W., Katuromunda, S. (2025). Physicochemical characteristics of effluent water from African catfish (*Clarias Gariepinus*) tanks fed fermented plant-based diets. *Trends in Ecological and Indoor Environmental Engineering, 4*(1), 60–69.
25. Oladosu, M. A., Abah, M. A., Odimgbe, E. I., Adewale, F. E., Arthur, C., Ajayi, A. S.,..., Ohanele, E. C. (2026). Smart electrochemical sensors and IoT for monitoring heavy metals in Nigerian water: review of advances and deployment challenges. *Trends in Ecological and Indoor Environmental Engineering, 4*(1), 79–89.
26. Onambele, N. L. N., Mouhaman, A., Ghogomu, R. T. (2025). Design of software for self-assessment of risks and environmental impacts. *Trends in Ecological and Indoor Environmental Engineering, 3*(3), 28–35.
27. Punyawansiri, S., Kwanyuen, B. (2020). Forecasting the future temperature using a downscaling method by LARS-WG stochastic weather generator at the local site of Phitsanulok Province, Thailand. *Atmospheric and Climate Sciences, 10*(4), 538–552.
28. Reyad, A., Fahad, A. T. (2025, November). An integrated hybrid life cycle assessment framework for evaluating the impact of wastewater sources on river water quality. In *IOP Conference Series. Earth and Environmental Science 1545*(1), 012056). IOP Publishing.
29. Riyadh, A., Hasan, R. F. (2026). Novel mathematical model for long-term hydrodynamic evolution of sediment transport and its impact on meandering geometry. *Journal of Water and Land Development*, 1–16.
30. Salman, S. A., Hamed, M. M., Shahid, S., Ahmed,

K., Sharafati, A., Asaduzzaman, M.,..., Dewan, A. (2022). Projecting spatiotemporal changes of precipitation and temperature in Iraq for different shared socioeconomic pathways with selected Coupled Model Intercomparison Project Phase 6. *Int. J. Climatol, 42*(16), 9032–9050.

31. Salman, S. A., Shahid, S., Ismail, T., Ahmed, K., Chung, E. S., Wang, X. J. (2019). Characteristics of annual and seasonal trends of rainfall and temperature in Iraq. *Asia-Pacific Journal of Atmospheric Sciences, 55*(3), 429–438.
32. Shehab, E. Q., Alsltany, R. (2025). A new approach to sustainable environmental assessment for wastewater treatment plants: A case study in the central region of Iraq. *Ecological Engineering & Environmental Technology, 26*.
33. Spiridonov, V., Ćurić, M., Novkovski, N. (2025). The planet under pressure: challenges in the twenty-first century. In: *Atmospheric Perspectives: Unveiling Earth's Environmental Challenges* (pp. 343–400). Cham: Springer Nature Switzerland.
34. Swart, N. C., Cole, J. N., Kharin, V. V., Lazare, M., Scinocca, J. F., Gillett, N. P.,..., Winter, B. (2019). The Canadian earth system model version 5 (CanESM5. 0.3). *Geoscientific Model Development, 12*(11), 4823–4873.
35. Wu, T., Yu, R., Lu, Y., Jie, W., Fang, Y., Zhang, J.,..., Shu, Q. (2020). BCC-CSM2-HR: A high-resolution version of the Beijing Climate Center Climate System Model. *Geoscientific Model Development Discussions, 2020*, 1–64.
36. Xu, Z., Yang, Z. L. (2017). Relative impacts of increased greenhouse gas concentrations and land cover change on the surface climate in arid and semi-arid regions of China. *Climatic Change, 144*(3), 491–503.